

# The MFM studies of the surface domain structure of Sm–Fe–Co–Zr–Cu thin ribbons

MARCIN DOŚPIAŁ<sup>1\*</sup>, MARCIN NABIAŁEK<sup>1</sup>, MICHAŁ SZOTA<sup>2</sup>, ŁUKASZ MICHTA<sup>1</sup>,  
PAWEŁ WIECZOREK<sup>2</sup>, KATARZYNA BŁOCH<sup>1</sup>, PAWEŁ PIETRUSIEWICZ<sup>1</sup>,  
KATARZYNA OŹGA<sup>3</sup>, JACEK MICHALCZYK<sup>4</sup>

<sup>1</sup>Institute of Physics, Częstochowa University of Technology,  
al. Armii Krajowej 19, 42-200 Częstochowa, Poland

<sup>2</sup>Institute of Materials Engineering, Częstochowa University of Technology,  
al. Armii Krajowej 19, 42-200 Częstochowa, Poland

<sup>3</sup>Institute of Electronics and Control Systems, Częstochowa University of Technology,  
al. Armii Krajowej 17, 42-200 Częstochowa, Poland

<sup>4</sup>Institute of Modeling and Automation of Plastic Forming Processes,  
Częstochowa University of Technology, al. Armii Krajowej 19, 42-200 Częstochowa, Poland

\*Corresponding author: [mdospial@wp.pl](mailto:mdospial@wp.pl)

The article contains studies of micro- and domain structures obtained using atomic/magnetic force microscopy (AFM/MFM) of melt-spun  $\text{Sm}_{12.5}\text{Fe}_8\text{Co}_{65.5}\text{Zr}_1\text{Cu}_{13}$  thin ribbons in the as-cast state. In order to obtain the  $\text{SmCo}_{8.5}$  type of structure in the Sm–Fe–Co–Zr–Cu alloy, thin ribbons were manufactured using the melt-spinning method with large linear velocity of a copper wheel and proper selection of alloying elements. The obtained samples in the as-cast state were magnetized. The microscopic results were also supported by magnetic measurements performed on a vibrating sample magnetometer as well as by a quantitative analysis of phase composition obtained using the Rietveld refinement method.

Keywords: atomic/magnetic force microscopy (AFM/MFM), surface domain structure, melt-spinning method, Sm–Co alloys, hard magnetic magnets.

## 1. Introduction

The latest interest has been focused on production methods and compositions of permanent magnets which can be used in elevated temperatures over 400 °C. To such a group of materials belong alloys on the basis of  $\text{Sm}(\text{Co}, \text{M})_{7-8.5}$  compounds, with the metastable type of structure. Conducted researches showed that the  $\text{SmCo}_{7-8.5}$  type of alloys next to high Curie temperature ( $T_C \sim 800$  °C) has lower intrinsic coercivity temperature coefficients ( $b = -0.10$  to  $-0.16\%$  °C<sup>-1</sup>) [1–3].

The  $\text{SmCo}_7$  type of metastable phase cannot steadily exist, therefore a third M element such as Si, Cu, Ga, Nb or Hf, *etc.*, is necessary to stabilize the structure [4]. The proper selection of a type and amount of M component can improve some of magnetic properties of fabricated alloys. If the electronegativity of the M additive element is less than that of Co, it prefers to occupy  $2e$  site of the crystal, otherwise, it tends to be at  $3g$  site. Furthermore, if the amount of an additive element is more than 3, M atoms prefer to occupy  $2c$  site [5]. If M occupies  $2e$  and  $3g$  sites, the anisotropy field of  $\text{SmCo}_{8.5}$  phase may increase, on the other hand it decreases if it occupies  $2c$  sites [6].

In this work, the microstructure and domain structure of the  $\text{Sm}_{12.5}\text{Fe}_8\text{Co}_{65.5}\text{Zr}_1\text{Cu}_{13}$  alloy in the form of as-cast ribbons were investigated.

## 2. Experimental procedure

The XRD patterns were carried out using a Bruker X-ray diffractometer with a  $\text{CuK}\alpha$  radiation source ( $\lambda \sim 1.541 \text{ \AA}$ ) and a scintillation counter. The quantitative and qualitative analysis of phase composition was carried out by analyzing the XRD patterns using the Rietveld profile matching method (Brass evaluation program [7]). The average grain size was estimated from Bragg's reflections with the highest intensities using the relation [8]:

$$\Delta^{hkl}(2\theta)\cos(\theta_B^{hkl}) = \frac{K\lambda}{D} + 2\frac{\Delta d}{d}\sin(\theta_B^{hkl}) \quad (1)$$

where:  $D$  – the grain size,  $K$  – the shape factor equal to 0.89,  $\lambda$  – the X-ray wavelength,  $\Delta^{hkl}$  – the line full width at a half maximum intensity (FWHM) in radians,  $\Delta d/d$  – the relative lattice strain, and  $\theta_B^{hkl}$  – the Bragg angle.

The magnetic measurements were performed by the LakeShore vibrating sample magnetometer with a maximum applied magnetic field of 2 T. From the hysteresis loop the magnetic parameters  $M_R/M_S$  ratio was derived.

The domain structure studies were carried out using magnetic force microscopy (MFM). The magnetic contrast imaging was performed in a tapping AFM/lift (MFM) mode. The signal was obtained by measuring the phase shift of an oscillating at resonant frequency cantilever. The MESP-ESP tip coated with Co–Cr films of thickness of  $\sim 35 \text{ nm}$  (nominal size, 50 nm maximum size) with coercivity of 32 kA/m and at a scan height of 100 nm was employed.

## 3. Results and discussion

Figure 1 presents the X-ray diffraction pattern and the results of simulation of Rietveld's refinement of the  $\text{Sm}_{12.5}\text{Fe}_8\text{Co}_{65.5}\text{Zr}_1\text{Cu}_{13}$  thin ribbon.

Bragg's reflections with the highest intensities observed on the XRD pattern were used to determine the average grain size. For each of the peaks the distribution

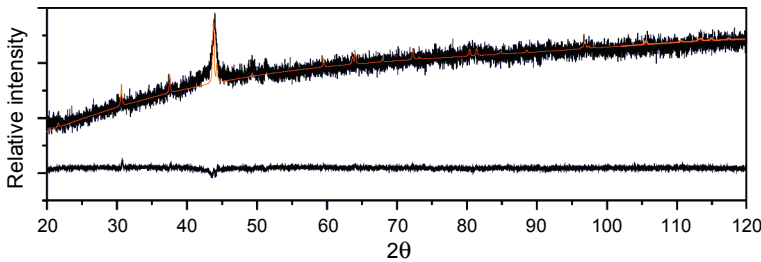


Fig. 1. X-ray diffraction pattern measured, calculated and the difference between them plotted from the Rietveld refinement, for the melt-spun  $\text{Sm}_{12.5}\text{Fe}_8\text{Co}_{65.5}\text{Zr}_1\text{Cu}_{13}$  thin ribbons in the as-cast state.

functions were fitted and FWHM and peak positions determined. In the next step these values were inserted into Eq. (1). The dependence (1) is linear and the grain size was calculated from the intersection of the straight line with the ordinate and was equal to 188 nm.

The quantitative and qualitative analysis of phase composition was carried out by the Rietveld profile matching method. The Rietveld refinement showed that the obtained alloy is only composed of the single  $\text{SmCo}_{8.5}$  type of phase. The fitting parameters were presented in Table 1.

Table 1. The Rietveld refinement fitting parameters.  $R_p$  – the primary factor,  $R_{wp}$  – weighted factor,  $R_{exp}$  – expected factor.

Assumed lattice parameters		Calculated lattice parameters		Obtained Rietveld coefficients		
<i>a</i>	4.7662 Å	<i>a</i>	4.7659 Å	$R_p$	$R_{wp}$	$R_{exp}$
<i>c</i>	4.0713 Å	<i>c</i>	4.0711 Å	1.91	2.55	0.08

The AFM structure is shown in Fig. 2a. This structure has large unbundlings, covered with a small bubble-like structure, what can be better seen in the magnified bright area in Fig. 2b. Through this area a test line was drawn. From the small fluctuation across the test line (Fig. 2c) the width distributions of bubble-like unbundlings were derived. This width was comparable with the size of grains determined from Eq. (1).

Figure 3a presents MFM domain structure pictures taken for the same area, for which AFM images were made (Fig. 2a).

From the observations of MFM pictures it can be concluded that the observed domain structures have a maze type of domain structure.

The domain width was determined using the stereologic method proposed by BODENBERGER and HUBERT [9–12], which is the most universal and commonly used method. In this method, an effective domain width is defined as the ratio of a chosen area to the total length of domain walls in this area. This definition of the domain width is in agreement with the ordinary definition for stripe domains with parallel straight

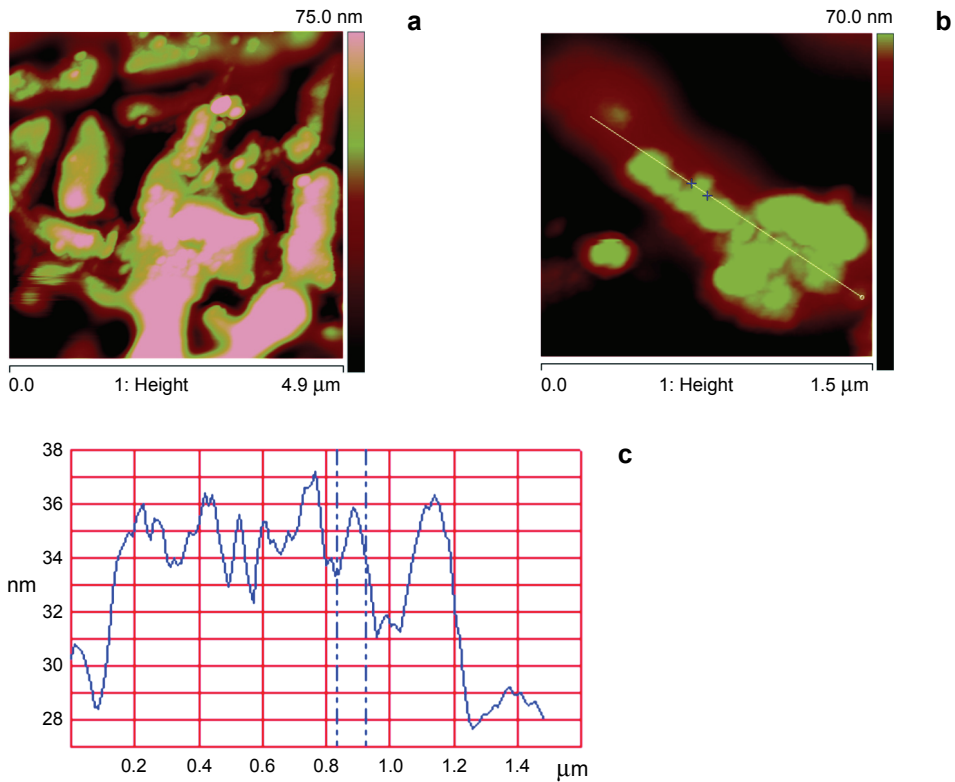


Fig. 2. AFM image of the surface (a), magnification of bright area with marked test line (b), width distribution of fine structure obtained from the small fluctuation across the test line for the melt-spun  $\text{Sm}_{12.5}\text{Fe}_8\text{Co}_{65.5}\text{Zr}_1\text{Cu}_{13}$  thin ribbons in the as-cast state.

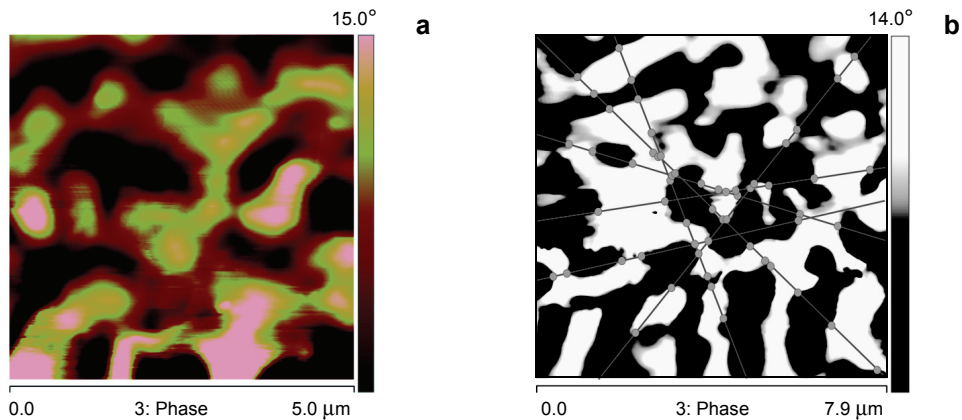


Fig. 3. Images of exemplary (a) MFM domain structure pictures taken for the same area, for which AFM images were made (Fig. 2a) and (b) domain structure with marked boundaries. Additionally, in the (b) images six exemplary test straight lines are superimposed to illustrate the stereologic method of Bodenberger and Hubert used for determining the domain width.

walls. In order to evaluate the total domain wall length, a large number of test straight lines running in random directions were drawn; the method is illustrated in Fig. 3b, where six test lines were drawn on each image. The surface domain width  $D_s$  is determined as:

$$D_s = \frac{2l}{\pi n} \quad (2)$$

where  $l$  is the total length of the test lines and  $n$  is the number of intersections of the test lines with domain walls.

From the relation (2) it was found that the average surface domain width was around 550 nm. That testifies to the fact that the observed structure is a multiple grain domain structure.

## 4. Conclusions

The quantitative and qualitative analysis of phase composition was carried out by the Rietveld profile matching method. The Rietveld refinement showed that the obtained alloy is only composed of the single  $\text{SmCo}_{8.5}$  type of phase. The average grain size estimated from ten Bragg's reflections with the highest intensities using the Scherrer relation was about 188 nm. These data were consistent with width distribution of a fine structure obtained from the small fluctuation observed at AFM pictures. The determined moderate grain size from grain size distributions observed on AFM pictures was about 120 nm ( $\pm 12$  nm [13]). Small differences in the moderate grain size resulted from the fact that X-ray diffractometry gave information from the entire volume of the sample and the AFM from the surface of the sample. The cooling speed of the surface during manufacturing ribbons is higher than cooling speed in the volume of the material, what results in smaller grain sizes on the surface of the material.

The MFM pictures were used to determine the domains width. It was found that the average surface domain width was around 550 nm. The observed multiple grain domain structure has a maze like character, typically met *inter alia* in nanomaterials with exchange interactions between grains.

The  $M_R/M_S$  ratio determined from a hysteresis loop was higher than 0.5 (0.61). In the case of permanent magnets this ratio can exceed this value only for anisotropic magnets or magnets where exchange interactions between grains are present.

*Acknowledgements* – This work was supported by the Ministry of Science and Higher Education of Poland through grant no. N N507 234940.

## References

- [1] DONGTAO T. ZHANG, MING YUE, JIU-XING X. ZHANG, LIJUN J. PAN, *Bulk nanocrystalline  $\text{SmCo}_{6.6}\text{Nb}_{0.4}$  sintered magnet with  $\text{TbCu}_7$ -type structure prepared by spark plasma sintering*, IEEE Transactions on Magnetism **43**(8), 2007, pp. 3494–3496.

- [2] CHANG H.W., HUANG S.T., CHANG C.W., CHIU C.H., CHANG W.C., SUN A.C., YAO Y.D., *Magnetic properties, phase evolution, and microstructure of melt spun  $\text{SmCo}_{7-x}\text{Hf}_x\text{C}_y$  ( $x = 0-0.5$ ;  $y = 0-0.14$ ) ribbons*, Journal of Applied Physics **101**(9), 2007, article 09K508.
- [3] CHENGBAO JIANG, VENKATESAN M., GALLAGHER K., COEY J.M.D., *Magnetic and structural properties of  $\text{SmCo}_{7-x}\text{Ti}_x$  magnets*, Journal of Magnetism and Magnetic Materials **236**(1–2), 2001, pp. 49–55.
- [4] DOŚPIAŁ M., NABIALEK M., SZOTA M., PLUSA D., *The magnetization reversal processes of  $\text{Sm}_2\text{Gd}_{10.5}\text{Fe}_8\text{Co}_{64}\text{Zr}_{2.5}\text{Cu}_{13}$  alloy in the as-quenched state*, Journal of Alloys and Compounds **509S**(Supplement 1), 2011, pp. S404–S407.
- [5] LUO J., LIANG J.K., GUO Y.Q., LIU Q.L., LIU F.S., ZHANG Y., YANG L.T., RAO G.H., *Effects of the doping element on crystal structure and magnetic properties of  $\text{Sm}(\text{Co}, \text{M})_7$  compounds ( $\text{M} = \text{Si}, \text{Cu}, \text{Ti}, \text{Zr}, \text{and Hf}$ )*, Intermetallics **13**(7), 2005, pp. 710–716.
- [6] GUO Y.Q., LI W., LUO J., FENG W.C., LIANG J.K., *Structure and magnetic characteristics of novel SmCo-based hard magnetic alloys*, Journal of Magnetism and Magnetic Materials **303**(2), 2006, pp. e367–e370.
- [7] BIRKENSTOCK J., FISCHER R.X., MESSNER T., *BRASS 1.0 beta: The Bremen Rietveld Analysis and Structure Suite*, Zentrallabor für Kristallographie und Angewandte Materialwissenschaften, Fachbereich Geowissenschaften, University of Bremen, 2003.
- [8] WILLIAMSON G.K., HALL W.H., *X-ray line broadening from filed aluminium and wolfram*, Acta Metallurgica **1**(1), 1953, pp. 22–31.
- [9] BODENBERGER R., HUBERT A., *Zur bestimmung der blochwandenergie von einachsigen ferromagneten*, Physica Status Solidi (A) **44**(1), 1977, pp. K7–K11, (in German).
- [10] HUBERT A., SCHÄFER R., *Magnetic Domains: the Analysis of Magnetic Microstructures*, Springer, Berlin, 1998, pp. 329, 386, 550.
- [11] PLUSA D., PFRANGER R., WYSŁOCKI B., *Dependence of domain width on crystal thickness in  $\text{YCo}_5$  single crystals*, Physica Status Solidi (A) **92**(2), 1985, pp. 533–538.
- [12] SZMAJA W., *Investigations of the domain structure of anisotropic sintered Nd–Fe–B-based permanent magnets*, Journal of Magnetism and Magnetic Materials **301**(2), 2006, pp. 546–561.
- [13] SEDIN D.L., ROWLEN K.L., *Influence of tip size on AFM roughness measurements*, Applied Surface Science **182**(1–2), 2001, pp. 40–48.

Received May 25, 2012  
in revised form November 16, 2012